High-cycle fatigue performance of Grade 600 steel reinforcing bars

Sourav Ray[1], Amin Heidarpour[1*], Mahsa Mirmomeni[2], Anthony Ng[3]
[1]Department of Civil Engineering, Monash University, VIC 3800, Australia
[2]Department of Business and Construction, Melbourne Polytechnic, VIC 3076, Australia
[3]InfraBuild Australia Pty Ltd, Sydney, NSW 2000, Australia

*Corresponding author: amin.heidarpour@monash.edu

Abstract: The mechanical behaviour of steel reinforcing bars under high-cycle fatigue (HCF) loading has gained attention over the last few decades. The reinforced concrete (RC) components of many structures, such as bridges, wind turbines, and offshore structures are subjected to HCF loading due to their operational loading from traffic, wind, waves, etc. High-strength steel (HSS) reinforcing bars have the potential to offer improved performance and sustainability by providing benefits such as reduced material consumption and steel congestion for RC structures, easier concrete placement, energy and resource conservation, as well as lower carbon footprint and transportation costs. However, very limited research has been conducted on the behaviour of HSS reinforcing bars under HCF loading. This research aims to explore the fatigue performance of 600 MPa HSS bars subject to HCF loading. The S-N relationship, representing the number of cycles to failure (N) at different stress ranges (S), were developed for Grade 600 S22 bars based on experimental results and compared to existing fatigue guidelines in different design standards. The results of the experimental tests presented in this paper can be regarded as the foundational step for the research on HSS reinforcing bars under fatigue loading conditions currently undertaken at Monash University.

Keywords: High-cycle fatigue, High-strength steel reinforcing bar, Fatigue test, Fracture surface, S-N relationship, Design standards

1. INTRODUCTION

The global trend towards higher-grade steel production enhances construction sustainability by offering benefits such as improved environmental performance, easier concrete placement due to reduced steel congestion, energy and resource conservation, and a lower carbon footprint [1]. This advancement is particularly valuable in constructing reinforced concrete (RC) structures, as these benefits contribute to improved overall performance and sustainability. High-strength steel (HSS) reinforcing bars are being manufactured across various countries, each adopting specific material standards to define their specifications. In the United States and Canada, HSS reinforcing bars include ASTM A706 Grade 550 and ASTM A1035 Grades 690 and 830 [2]. Japan classifies its HSS reinforcing bars as USD685A and USD685B [2] for seismic-resistant infrastructure, while China has developed HTRB630, a heat-treated ribbed bar ensuring improved durability and strength [3]. The latest revisions of AASHTO LRFD Bridge Design Specifications (2020) [4] and ACI 318-19 code [5] have officially included Grade 100 (690 MPa) reinforcing steel bars in their specifications. The revisions to Australian standards AS 3600 – Concrete structures (2018) and AS/NZS 4671 – Steel for the reinforcement of concrete (2019) have increased the permissible maximum yield strength of steel reinforcing bars [6, 7]. The latest edition of AS 3600 (2018) permits the use of steel reinforcing bars as longitudinal reinforcement with yield strength of up to 600 MPa and as column fitments up to 800 MPa [6,8 –10]. Furthermore, the second amendment to the Australian Standard AS 5100.5 – Bridge design, Part 5: Concrete, published in May 2024 [11], now permits the use of 600 MPa reinforcing steel bars, aligning it with both AS 3600 and AS/NZS 4671 [6,7]. These changes have created new opportunities for the reinforced concrete industry to utilise the benefits offered by higher-grade steel reinforcing bars in the design and construction of concrete structures including RC bridges.

However, it is crucial to recognize that many RC structures, including bridges, wind turbines, and offshore structures, face high-cycle fatigue (HCF) loading challenges due to operational loads from traffic, wind, and other forces. HCF occurs when a material is subjected to a large number of load cycles with small elastic strains at relatively low-stress levels before failure [12]. Fatigue loads can lead to premature failures in steel bars of RC structures, often without visible structural damage beyond local concrete cracking [13]. Therefore, to capitalize on the benefits of HSS bars, it is essential to verify their compatibility to be used in fatigue-prone structures, including bridges and wind turbines, etc. With the recognition of the production and use of 600 MPa reinforcing steel by Australian Standards, InfraBuild, the only manufacturer of steel reinforcing bars in Australia, has introduced high-strength, normal ductility 600 MPa grade steel reinforcing bars, branded SENSE 600®. These bars are designed with non-standard diameters that offer an equivalent design capacity to the standard diameter 500 MPa bars already available in the Australian market [8,10]. The equivalent design capacity diameter concept simplifies the substitution of 600 MPa steel bars for existing 500 MPa bars without changing the quantity or arrangement within the structural members [8 –10]. While these bars provide benefits in terms of reduced material mass and embodied carbon [14,15], as well as satisfactory performance as longitudinal reinforcement in concrete elements for non-fatigue applications [9,15], the lack of research data on these Australian-made HSS reinforcing bars limits their potential for use in fatigue-prone structures. Furthermore, existing research on HCF performance of steel reinforcing bars has primarily focused on normal-strength steel bars with characteristic yield strengths of 500 MPa or lower [16–22]. In contrast, studies investigating HSS bars (characteristic yield strength ≥ 600 MPa) under HCF conditions remain very limited [3,23]. Therefore, fundamental research is necessary to understand the HCF performance of Australian-made 600 MPa bars to realise their full potential and ensure their safe and effective application in fatigue-prone structures.

Extensive research is underway at Monash University to evaluate the fatigue response of 600 MPa HSS reinforcing bars manufactured in Australia subjected to HCF loading. This paper presents the HCF behaviour of 600 MPa S22 (21.6 mm diameter) steel bars. The findings of this initial study can be regarded as the foundational step for the research on Australian made 600 MPa steel bars. Furthermore, the paper evaluates the performance of 600 MPa S22 bars against the fatigue verification criteria for steel bars in the existing Australian and international design standards for design of RC structures.

2. EXPERIMENTAL PROGRAM

2.1 Material properties

Australian-made 600 MPa high-strength steel reinforcing bars, are quenched and self-tempered (QST) steel bars manufactured in accordance with AS/NZS 4671:2019 [7]. In this study, 600 MPa S22 steel bars with a nominal diameter of 21.9 mm were used. Monotonic tensile tests were conducted on 600 MPa S22 using a Instron 600DX testing system at a constant crosshead speed of 2 mm/min (Figure 1). Strain during the static tension test was recorded using MTS LX500 laser extensometer. The results of tensile testing of bars are presented in Table 1.

Table 1. Tensile properties of 600 MPa S22 as-received steel bar

Specification	Nominal diameter (mm)	f_y (MPa)	f_u (MPa)	f_u/f_y
S22	21.9	607	711	1.17

f_y = yield strength, f_u = ultimate tensile strength

The yield strength of the S22 bars, measured at 607 MPa, exceeds the characteristic yield strength of 600 MPa. The tensile strength to yield strength ratio (f_u/f_y) is 1.17 for 600 MPa S22 bars and thus fulfills the ductility requirement of f_u/f_y>1.08 for normal ductility (class N) bars according to AS/NZS 4671:2019 [7]. Rockwell hardness (HRC) of the steel bar specimen was also measured and compared with a 500 MPa N24 using a Zwick Roel RH-150 AUTO portable Rockwell hardness tester. The hardness was measured across the cross-sectional profile of the specimens in the radial direction, from the edge of the bars to the centre. A reduction in Rockwell hardness value from the outer edge region to the centre of the bar is observed (Figure 1) for both S22 and N24 bars, indicating a hard self-tempered martensitic layer at the edge and a softer core [20,21].

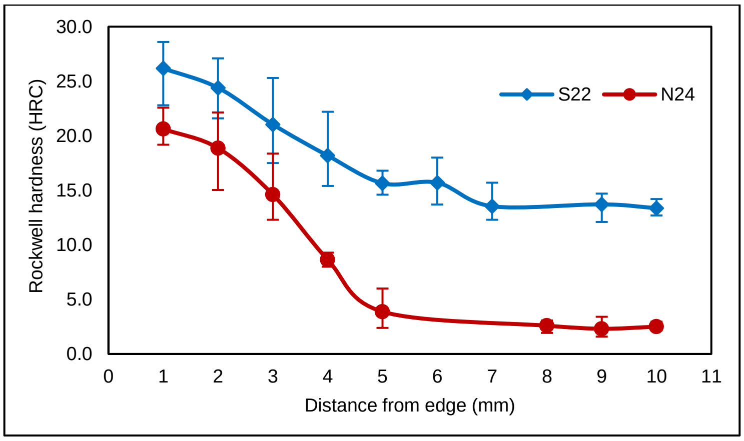

Figure 1. Rockwell hardness of S22 and N24 bars

S22 bars show a superior hardness profile across the entire cross-sectional profile compared to N24 bars. The superior hardness profile of S22 bars may be attributed to the differences in production process, cooling time and rate, any specific composition of alloying elements, and higher compressive residual stress at the surface, etc. [24–27]. Further microstructural analysis will be conducted to depict the phase distribution of the bars more precisely across the cross-section.

2.2 High-cycle fatigue test

HCF tests were performed on as-received S22 steel bar specimens using a 250 kN capacity Instron 8802 servo-hydraulic testing system accordance with ISO 15630-1[28]. A sinusoidal constant-amplitude alternating load with a frequency of 20 Hz was applied to the test specimens in air, each measuring 600 mm in length. According to ISO 15630-1 , the free length of the axial fatigue test specimens should be at least 140mm or 14 times the specimen diameter, whichever is greater. In this study, the grip length at both the top and bottom ends and the free length of specimens were taken as 90 mm and 420 mm, respectively satisfying the requirements of ISO 15630-1. For the majority of the fatigue tests, a stress ratio (R=minimum stress/maximum stress) of R=0 was used. Additionally, a number of preliminary tests were conducted with R=0.125 and R=0.20. The tests were continued until specimen fracture or achieving a very high number of cycles; e.g. two tests on S22 bars were extended to over 18 million cycles. Test results were considered valid only if the specimens did not fail at the grip or within a distance of 2-bar diameters from the grip [28].

2.3 Preparation of test specimen and grip arrangement

During the axial fatigue test on bare bars in air, premature facture of the test specimens may occur at or within the grip region due to stress concentration and stress triaxiality resulting from the gripping pressure, thereby compromising the validity of the test in accordance with ISO 15630-1 .To address this issue, the clamping ends of the bars were wrapped with a CFRP sheet (SikaWrap 230C) using an epoxy adhesive (Sikadur 330) as the bonding agent and cured at ambient temperature for at least 72 hours. After the epoxy adhesive had sufficiently cured and dried, the CFRP-wrapped ends were machined to ensure a smooth surface and thereby reduce stress concentrations on the gripping ends of the specimens (Figure 2). This modified arrangement resulted in more valid test outcomes due to the more uniform distribution of forces across the gripped sections of the bars.

(a) (b)

Figure 2. Fatigue test specimen preparation: (a) CFRP sheet, (b) CFRP wrapped machined bar ends

3 RESULTS AND DISCUSSION

3.1 High-cycle fatigue response of 600 MPa S22 bars

A total of 14 axial fatigue tests were conducted at 12 stress levels for S22 bar specimens at a stress ratio of R=0. Four tests were invalid, as the bar specimens fractured near or within the grip region, while eight tests were valid. Two specimens at 30% and 40% of f_y stress levels surpassed 18 million cycles without failure. Moreover, a single test for R=0.125 and two tests for R=0.2 were considered for initial assessment of the stress ratio effect on fatigue performance at the same stress level, and all tests were valid (Figure 3).

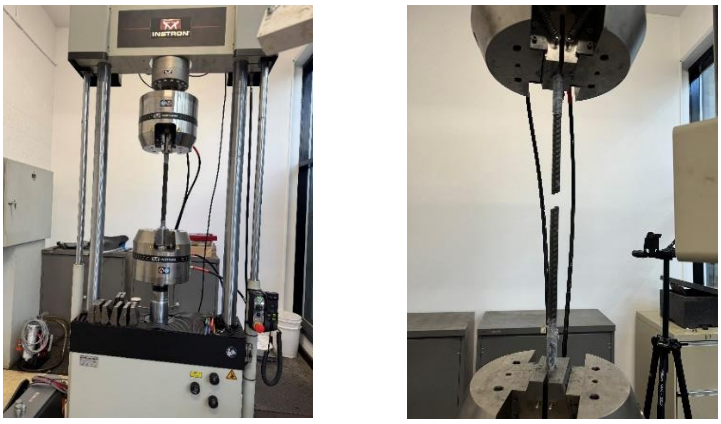

(a) (b)

Figure 3. High-cycle fatigue test of steel bar – (a) Instron 8802 testing system, (b) a typical valid fatigue test

The fatigue test data is usually expressed by the S-N relationship, representing the number of cycles to failure (N) at different stress ranges (S). The mean S-N curve with a 50% survival probability [29], based on the Basquin relation, can be expressed as shown in Eqn. (1).

$$\log \mathrm{N} = \log \mathrm{C} - \mathrm{m} \log \mathrm{S} \tag{1}$$

log C and *m* are constants which can be obtained from a linear least square regression analysis.

The S-N relationship is plotted for Grade 600 S22 reinforcing steel based on experimental results for all stress ratios tested, as shown in Figure 4. The mean S-N curve equation for S22 bars for R=0 is shown in Eqn. (2).

$$\log N = 16.763 - 4.497 \log S \tag{2}$$

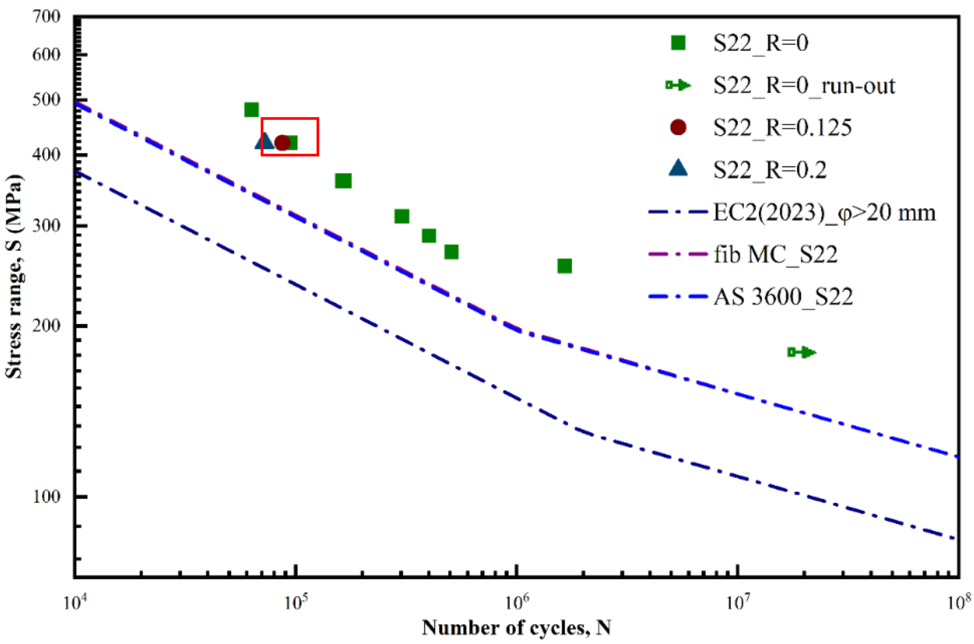

Figure 4. S-N relationship for Grade 600 – S22 bars

Figure 4 and Table 2 show that the fatigue life for S22 bars decreases with increasing stress ratio (R).

Table 2 Fatigue life of S22 bars at different stress ratios

Stress ratio, R	Stress range, S MPa	No. of cycles to failure, N
0	420.0	94,573
0.125	420.0	87,000
0.20	420.0	71,837
	420.0	72,651

In this study, the stress range was kept constant for different stress ratios, resulting in higher mean stress at higher maximum and minimum stress levels for increased stress ratios. The increase in tensile mean stress might accelerate fatigue crack propagation and consequently reduce fatigue life [30].

3.2 High-cycle fatigue fracture surface

The fracture surface of S22 bars under HCF loading is shown in Figure 5. From a macroscopic view, two distinct regions have been identified in the fracture surface of the S22 bars. Among the two distinct fracture surface zones, the relatively smooth surface region is called the crack propagation zone or fatigue fracture zone, and the coarser and rough fracture surface region is known as the fast fracture region or transient breaking zone [3,20].

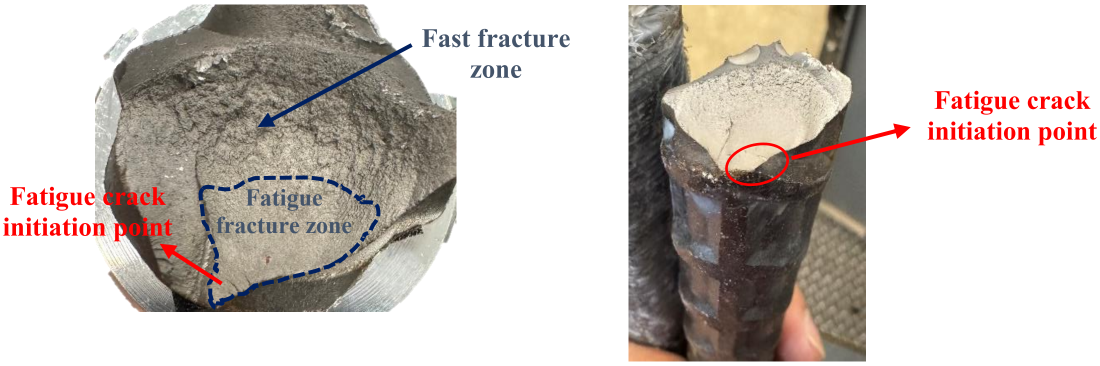

Figure 5. Fatigue fracture surface of S22 steel bars

From Figure. 5, it can be observed that fatigue cracks initiate on the surface of the 600 MPa S22 bars, specifically at the root of the transverse rib. Researchers [31,32] have reported high stress concentrations on the bar surface, particularly around the transverse rib root region. The crack initiation point is located at or close to the intersection of the longitudinal and transverse ribs. Therefore, the fatigue crack initiation may be influenced by the proximity to the rib intersection zone due to higher stress concentration around the zone.

3.3 Comparison of S-N relationship with design standards

The S-N relationship of Grade 600 S22 reinforcing steel bars based on experimental results are compared to existing fatigue guidelines in different design standards, namely, Eurocode 2: 2023 [33], fib Model Code: 2020 [34], and AS 3600 (2018), as shown in Figure 4. It can be observed that the fatigue performance of 600 MPa S22 bars exceeds the performance recommended by the different design standards, demonstrating safe fatigue performance. Among these design standards, Eurocode 2 is found to be overly conservative.

Table 3 Comparison of fatigue strength of 600 MPa S22 bars with design standards

Source	Fatigue strength (MPa)	
	$N = 1 \times 10^6$	Relative strength
SENSE 600®_S22	247.3	1.00
EC 2 (2023)_φ>16 mm	149.3	0.60
fib MC (2020)_S22	197.7	0.80
AS 3600 (2018)_S22	196.2	0.79

Table 3 presents the fatigue strength of S22 bars based on experimental data and various design standards at 1 million cycles. It can be observed that the design standards predict the fatigue strength ranging from 60% to 79% of the experimentally obtained fatigue strength of S22 bars.

3.3.1 Testing to Facilitate Changes to AS 5100.5:2017 Bridge design, Part 5: Concrete

Each diameter in the range of Australian-made 600 MPa HSS reinforcing bars is equivalent in design capacity to a 500 MPa bar to allow for easy one-for-one substitution of bars. This means each 600 MPa steel reinforcing bar is 20% smaller in area compared with its equivalent capacity 500 MPa steel reinforcing bar and therefore when subjected to the same load, the stress in the 600 MPa bar will be 20% higher. This study on the HCF loading of the 600 MPa bar should take this into account to facilitate the one-to-one substitution of the 500 MPa bar in design.

According to the Australian Bridge design standard, AS 5100.5: 2017 [35], straight steel reinforcing bars must withstand 2 million cycles at a tensile stress range of 150 MPa to satisfy fatigue design criteria. Therefore, the Australian-made 600 MPa HSS reinforcing bars considers a minimum stress range of 180 MPa (≥30% of characteristic f_y), which is 20% higher than the 150 MPa stress range that would typically be used in design for 500 MPa bars.

Experimental results show that 600 MPa S22 bars surpassed 18 million and 19 million cycles without failure under stress ranges of 180 MPa and 240 MPa, respectively. Therefore, the initial results for 600 MPa, S22 bars met the objectives of the study. That is, the number of fatigue cycles at a design stress level 20% higher than the requirements for steel reinforcing bar in AS 5100.5:2017 were exceeded.

4. CONCLUSION

Determining the behaviour of Australian-made Grade 600 high-strength steel reinforcing bars under high-cycle fatigue loading is critical for their efficient application in fatigue-sensitive structures. This study evaluated the fatigue response of Grade 600 steel bars under constant-amplitude axial fatigue testing. The key findings from the experimental investigations are summarized as follows:

i. The S-N relationship for Grade 600 S22 reinforcing steel bars was established based on experimental results for all stress ratios. The fatigue life for S22 bars decreased with increasing stress ratio (R). This reduction in fatigue life can be attributed to the increase in tensile mean stress at higher stress ratios, which accelerates fatigue crack propagation.
ii. Wrapping the clamping ends of the bars with a CFRP sheet using an epoxy adhesive and machining the wrapped ends to achieve a smooth surface resulted in more valid tests. This approach ensured a uniform distribution of force across the gripped section of the bars.
iii. The fatigue fracture surface of 600 MPa S22 bars constitutes two distinct regions: a smooth crack propagation zone and a rough fast fracture zone. Fatigue cracks initiated at or close to the intersection of the longitudinal and transverse ribs.
iv. The fatigue performance of 600 MPa bars met the fatigue design requirements recommended by the different design standards, namely, Eurocode 2 (2023), fib Model Code (2020), AS 3600 (2018), and AS 5100.5 (2017), demonstrating safe fatigue performance of 600 MPa S22 bars in fatigue sensitive reinforced concrete structures.

5. FUTURE WORK

The results of the experimental tests presented in this paper sets the foundation for the research on HSS reinforcing bars under fatigue loading. Significantly more testing is planned at Monash Universtiy at the lower stress levels where designs are typically required to withstand fatigue cycles from $2x10^6$ up to $1x10^8$. Testing is proposed for a range of 600 MPa steel reinforcing bars to investigate the impact of the bar diameter on the fatigue life with a view to develop design curves for the proprietary Australian Made 600 MPa steel reinforcing bar.

6. ACKNOWLEDGEMENTS

The authors extend their appreciation to InfraBuild Trading Pty Ltd for supplying the bars. They also acknowledge the support of the Monash Civil Engineering technical staff during the experimental testing.

7. REFERENCES

1. A. Heidarpour, F. Javidan, D.A. Truong, Performance of High-Strength Steel Reinforcing Bars under Low- Velocity Impact, in: Concrete Institute of Australia’s Conference: Concrete 2023, Perth, Australia, 2023.

2. S. Aldabagh, M.S. Alam, High-Strength Steel Reinforcement (ASTM A1035/A1035M Grade 690): State-of-the-Art Review, J. Struct. Eng. 146 (2020) 03120003. https://doi.org/10.1061/(ASCE)ST.1943-541X.0002720.
3. C. Sun, M.-L. Zhuang, Z. Wang, L. Gao, M. Hou, Y. Qiao, W. Zhang, Experimental and Numerical Investigations of High-Cycle Fatigue Properties of HTRB630 High-Strength Steel Bars, J. Mater. Civ. Eng. 35 (2023) 04023222. https://doi.org/10.1061/JMCEE7.MTENG-15172.
4. AASHTO, AASHTO LRFD Bridge design specifications, (2020).
5. ACI 318, Building code requirements for structural concrete (ACI 318-19) and commentary, (2019).
6. AS 3600, Concrete Structures, Standards Australia, Sydney, Australia, (2018).
7. AS/NZS 4671, Steel for the reinforcement of concrete, Standards Australia, Sydney, Australia, (2019).
8. D. Drevon, M. Holt-Smith, Ng, Anthony, J. Brown, 600 MPa Prefabricated Column Cages to Improve Sustainability, in: Australasian Structural Engineering Conference: ASEC 2024, Melbourne, Australia, 2024.
9. A. Ng, G. McGregor, High strength reinforcing steels: The benefits and how they are delivered, in: Australian Structural Engineering Conference: ASEC 2020, 2020: pp. 56–67.
10. A. Ng, S.J. Foster, McGregor, Graeme, The impact of confinement and time effects on the calculated squash load of concrete columns reinforced with 600 MPa steels, in: Concrete Institute of Australia's Conference: Concrete 2023, Perth, Australia, 2023.
11. AS 5100.5:2017 Amd 2:2024, Australian bridge design specifications, (2024).
12. T. Nicholas, High cycle fatigue: a mechanics of materials perspective, Elsevier, 2006.
13. X.-W. Sheng, W.-Q. Zheng, Y. Yang, Tensile and high-cycle fatigue performance of HRB500 high-strength steel rebars joined by flash butt welding, Construction and Building Materials 241 (2020) 118037.
14. A. Ng, McGregor, Graeme, J. Merrick, The curvilinear stress block-a design model to decarbonize reinforced concrete columns using 600 MPa steels., in: Australasian Structural Engineering Conference: ASEC 2022, Melbourne, Australia, 2022: pp. 27–36.
15. A. Ng, McGregor, Graeme, S.J. Foster, H.V.P. Goudazi, Customised rib pattern to reduce development lengths for 600 MPa reinforcing steels, in: 2024.
16. K.J. Byun, H.W. song, L. Noh Byeong Cheol, J.-S. Yang, Experimental Study on Fatigue Characteristics of Reinforcing Bars, Proceedings of the Korea Concrete Institute Conference (1996) 312–316.
17. K.J. Byun, B.C. Lho, H.W. song, Experimental Study on Fatigue Characteristics of Domestic Reinforcing Bars, Magazine of the Korea Concrete Institute 9 (1997) 177–187. https://doi.org/10.22636/MKCI.1997.9.5.177.
18. J. Fei, D. Darwin, Fatigue of high relative rib area reinforcing bars, Federal Highway Administration: Lawrence, KS, USA, 1999.
19. T. Helgason, J.M. Hanson, N.F. Somes, W.G. Corley, E. Hognestad, Fatigue strength of high-yield reinforcing bars, Nchrp Report (1976). https://trid.trb.org/View/46449 (accessed July 26, 2024).
20. S.K. Paul, P.K. Rana, D. Das, S. Chandra, S. Kundu, High and low cycle fatigue performance comparison between micro-alloyed and TMT rebar, Construction and Building Materials 54 (2014) 170–179.
21. M. Rocha, S. Michel, E. Brühwiler, A. Nussbaumer, Very high cycle fatigue tests of quenched and self-tempered steel reinforcement bars, Mater Struct 49 (2016) 1723–1732. https://doi.org/10.1617/s11527-015-0607-5.
22. H. Zheng, A.A. Abel, Fatigue Properties of Reinforcing Steel Produced by TEMPCORE Process, J. Mater. Civ. Eng. 11 (1999) 158–165. https://doi.org/10.1061/(ASCE)0899-1561(1999)11:2(158).

23. J.-H. Lee, S.-H. Lee, H.-Y. Kim, Fatigue Strength of High Strength Reinforcing Bars Having Yield Strength of 700MPa, Korea Concrete Institute 30 (2018). https://doi.org/10.4334/JKCI.2018.30.3.269.
24. E. Ahmed, S. Ibrahim, M. Galal, S.A. Elnekhaily, T. Allam, Microstructure and Mechanical Properties of V-Alloyed Rebars Subjected to Tempcore Process, Metals 11 (2021) 246. https://doi.org/10.3390/met11020246.
25. A. Fry, Residual stresses in materials at high temperature: the Link to hardness and scale exfoliation (NPL Report MN 5), National Physical Laboratory, Middlesex, United Kingdom, 2009.
26. E. Mansutti, G. Luvarà, C. Fabbro, N. Redolfi, Microstructural characterization and production of high yield strength rebar, La Metallurgia Italiana (2015).
27. K. Tosha, Influence of residual stresses on the hardness number in the affected layer produced by shot peening, in: 2002: pp. 48–54.
28. ISO 15630-1, Steel for the Reinforcement and Prestressing of Concrete-Test Methods-Part 1: Reinforcing Bars, Wire Rod and Wire, (2019).
29. L. Ke, F. Zhu, Z. Chen, Z. Feng, J. Zhou, Y. Li, Fatigue failure mechanisms and probabilistic S-N curves for CFRP–steel adhesively bonded joints, International Journal of Fatigue 168 (2023) 107470. https://doi.org/10.1016/j.ijfatigue.2022.107470.
30. G.P. Tilly, Fatigue of Steel Reinforcement Bars in Concrete: A Review, Fatigue & Fracture of Engineering Materials & Structures 2 (1979) 251–268. https://doi.org/10.1111/j.1460-2695.1979.tb01084.x.
31. S. Rappl, K. Osterminski, Notch stress analysis on reinforcing steel bars using FE-Simulations considering surface topography and structure properties, in: Current Perspectives and New Directions in Mechanics, Modelling and Design of Structural Systems, CRC Press, 2022.
32. M. Rocha, E. Brühwiler, A. Nussbaumer, Geometrical and Material Characterization of Quenched and Self-Tempered Steel Reinforcement Bars, Journal of Materials in Civil Engineering 28 (2016) 04016012. https://doi.org/10.1061/(ASCE)MT.1943-5533.0001355.
33. B. Standard, Eurocode 2: Design of concrete structures, Part 1 (2023) 230.
34. International Federation for Structural Concrete, ed., Fib model code for concrete structures (2020), Version 1, Fédération internationale du béton - International Federation for Structural Concrete (fib), Lausanne, 2023.
35. AS 5100.5:2017, Australian bridge design specifications, (2017).